ELSEVIER

Ceramics International 31 (2005) 115–119

CERAMICS INTERNATIONAL

www.elsevier.com/locate/ceramint

Preparation and electrical properties of $La_{0.4}Sr_{0.6}Ni_{0.2}Fe_{0.8}O_3$ using a glycine nitrate process

Guangyan Zhu, Xiaohong Fang, Changrong Xia*, Xingqin Liu

Laboratory for Biomass Clean Energy, Department of Materials Science and Engineering, University of Science and Technology of China, Hefei 230026, PR China

Received 24 November 2003; received in revised form 12 December 2003; accepted 24 March 2004
Available online 26 June 2004

Abstract

Perovskite structured $La_{0.4}Sr_{0.6}Ni_{0.2}Fe_{0.8}O_3$ (LSNF) powder was prepared by a glycine nitrate process (GNP). The electronic conductivity of LSNF was investigated using a four-probe technique. The crystal structure of GNP-derived LSNF was analyzed with X-ray diffraction. The possibility of using LSNF as cathodes for solid oxide fuel cells (SOFCs) was investigated in symmetric cells at temperature between 500 and 850 °C. The interfacial polarization resistance between LSNF cathodes and samaria-doped ceria (SDC) electrolyte was studied by impedance measurement. The effect of firing temperature and SDC addition on the interfacial resistance was systematically studied. Results show that the optimum firing temperature is about 950 °C, whereas the optimum amount of SDC addition is about 45 vol.% in the LSNF–SDC composite; polarization resistances for this LSNF–SDC cathode was as low as 0.16 Ω cm^2 at 700 °C and 0.06 Ω cm^2 at 800 °C, indicating LSNF is a promising cathode for intermediate temperature SOFCs based on doped ceria electrolytes.
© 2004 Elsevier Ltd and Techna S.r.l. All rights reserved.

Keywords: C. Impedance; D. Perovskites; E. Fuel cells; E. Electrodes

1. Introduction

Solid oxide fuel cells (SOFCs) have attracted much attention for their distinguished advantages comparing to other types of fuel cells, such as high-efficiency, high-quality exhaust heat, and system compactness. However, conventional SOFCs operating at high temperature up to 1000 °C, which causes many problems including electrode sintering, interfacial diffusion between electrolytes and electrodes, and highly cost materials such as La(Sr)MnO_3 and La(Sr)CrO_3 [1,2]. These obstruct the commercialization of SOFCs. If the operating temperature is reduced to 800 °C and lower, the cost for materials and operation can be reduced greatly by using cheaper materials, such as metallic interconnectors and by prolonging SOFCs operating life. As the temperature is lowered, however, the electrochemical processes at the cathode decreases, limiting SOFC performance, thus much work has been recently conducted on developing high-performance cathode materials for low-temperature cathodes.

It has been widely accepted that the cathode of SOFCs should have high-electronic and ionic conductivities, adequate porosity for gas transport, thermal and chemical compatibilities with the electrolyte, and long-term stability [1,3,4]. Therefore, interest is currently being expressed in Mixed Electronic and Ionic Conductors (MIECs), such as perovskite oxides with high conductivities. Perovskite type oxides (ABO_3) containing Co ions in B sites have much higher electronic and ionic conductivities than the most commonly used materials $La_{1-x}Sr_xMnO_3$ [5]. But the thermal expansion coefficients (TEC) of those materials are much larger ($22 \times 10^{-6}\,k^{-1}$) than that of electrolytes ($10.6 \times 10^{-6}\,k^{-1}$) [1]. Recently, $La_{0.8}Sr_{0.2}FeO_3$ (LSF) has been developed as cathode materials for intermediate temperature (600–800 °C) SOFC. Simner et al. demonstrated that when LSF is used as cathode SOFC has high-power outputs (~0.9–0.95 W/cm^2 at 750 °C in air) and long-term stability (770 mW/cm^2 at 0.7 V, 700 °C with no discernible degradation over a 500 h period) [6]. But, its relative low-electronic conductivity limits further improvements

* Corresponding author. Tel.: +86-551-3607475; fax: +86-551-3606689.
E-mail address: xiacr@ustc.edu.cn (C. Xia).

0272-8842/$30.00 © 2004 Elsevier Ltd and Techna S.r.l. All rights reserved.
doi:10.1016/j.ceramint.2004.03.042

of LSF-based cathode since the performance is significantly reduced when a portion of LSF is replaced with electrolyte, such as doped ceria. It is known that $LaNiO_3$ has a very high-electronic conductivity at room temperature. However, $LaNiO_3$ is unstable above 850 °C, where it decomposes to La_2NiO_4 and NiO. Recently, Hrovat et al. showed that $LaNiO_3$ was stable at high temperature when some of the Ni is substituted by Co [7]. When Fe is used as substitution, it was also shown that this material is stable at high temperature, for example, $La_{1-y}Sr_yNi_{1-x}Fe_xO_3$ is stable up to 1400 °C. When the Fe fraction is higher than 0.5, the material has a high-electronic conductivity ($La_{0.6}Sr_{0.4}Ni_{0.2}Fe_{0.8}O_3$ 435 S/cm at 800 °C) and a TEC close to that of zirconia and ceria electrolytes [8,9]. The high conductivity, TEC matched to electrolytes, and thermal stability of $La_{1-y}Sr_yNi_{1-x}Fe_xO_3$ make this material a potential cathode for SOFCs. In this study, the possibility of $La_{0.4}Sr_{0.6}Ni_{0.2}Fe_{0.8}O_3$ as cathode for SOFC with samaria-doped ceria electrolyte was investigated using AC impedance measurement.

2. Experiments

2.1. Powder synthesis and characterization

$La_{0.4}Sr_{0.6}Ni_{0.2}Fe_{0.8}O_3$ (LSNF) and $Sm_{0.2}Ce_{0.8}O_{1.9}$ (SDC) powders were prepared using glycine nitrate combustion technique (GNP) [10]. For example, to prepare LSNF, nitrate salts of La, Sr, Ni, and Fe were dissolved in distilled water with a molar ratio of 4:6:2:8. Glycine, 1.4 times to the total mole amount of metal ions, was then added to the solution. The solution was subsequently dried to form gel, heated to combustion, and calcined at 900 °C for 2 h to remove the residual carbon and to form the perovskite structure. The powder was ball milled with zircite balls for 24 h to break agglomeration. The crystal structure of the powder was analyzed with X-ray diffraction (XRD) using a PHILIPS X'Pert Pro Super using Cu Kα (1.541874 Å) as the target.

2.2. Electronic conductivity

The powder was uniaxially pressed into rods (30.0 mm × 6.3 mm × 1.8 mm), sintered at 1200 °C for 3 h. Ag leads were attached to the sintered rods with Ag paste and fired at 800 °C for 30 min. Conductivity in air from 500 to 800 °C was measured using DC four-terminal method with an HP34401 AMULTIMETER impedance analyzer.

2.3. Sample preparation

SDC pellets of about 1 mm thick and 12 mm in diameter were prepared by uniaxially pressing of SDC powder, which was synthesized by oxalate coprecipitation [11]. The pellets were subsequently sintered at 1450 °C for 5 h in air. The density of the pellets was 95–98% of theoretical density as measured by standard Archimedes method. To prepare the composite cathodes, the GNP-derived LSNF and SDC powders were mixed by ball milling for 24 h. The weight ratio of LSNF to SDC was set to be 65:35, 57:43, 55:45, 50:50, and 47:53. In this paper, the composite cathodes will be identified by the wt.% (measured) or by the vol.% (calculated) obtained form the wt.% of the SDC. The volume fraction is about 4.4% lower than the wt.%. The mixed powders were then dispersed in an organic binder consisting of terpineol, and ethanol by dipping the SDC pellets into the slurry, drying the coating layers, and firing at 950 °C for 5 h in air. Surface and cross-section of the cathode were observed by scanning electron microscopy (SEM, Hitachi X-650). The electrode responses at temperature from 500 to 800 °C were measured using CHI604A with an applied potential of 20 mV and over the frequency range 0.001 Hz–0.1 MHz using the symmetrical two-electrode cell as schematically shown in Fig. 1. The two identical electrodes are applied on each side of a SDC pellet and tested simultaneously, and data were measured 30 min after the cells reached the desired temperature.

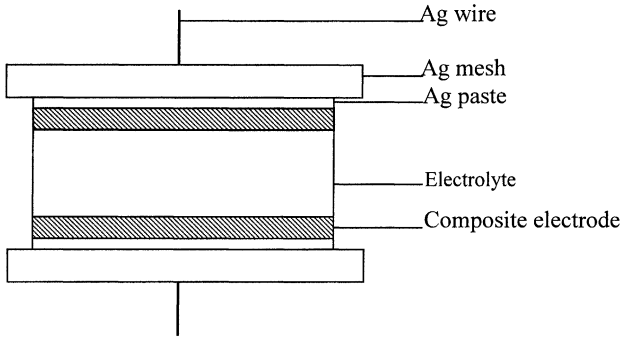

Fig. 1. The scheme of a symmetrical two-electrode measurement cell.

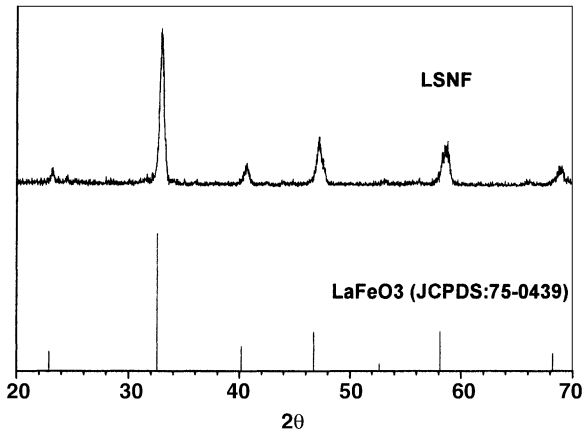

Fig. 2. X-ray diffraction for GNP-derived LSNF powder fired at 900 °C for 2 h.

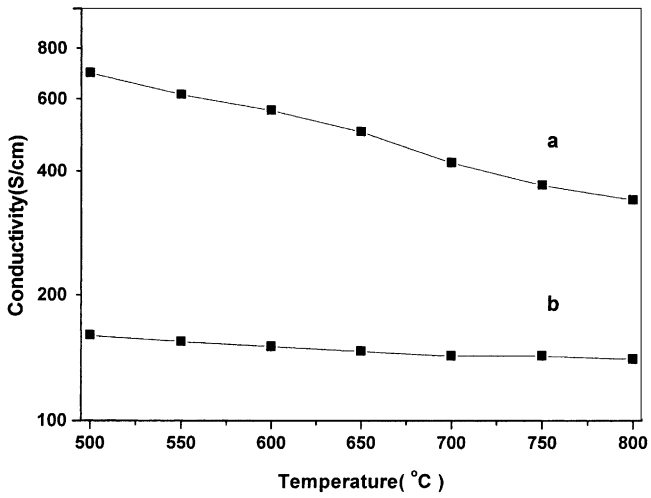

Fig. 3. Dependence of electrical conductivity on temperature for LSNF with (a) 3% porosity [8] and (b) 34% porosity.

3. Experimental results and discussion

3.1. Crystal structure and electrical conductivity of GNP-derived LSNF

The X-ray diffraction patterns for GNP-derived LSNF powder fired at 900 °C for 2 h are shown in Fig. 2. A perovskite $LaFeO_3$ (JCPDS: 75-0439) is also shown in Fig. 2 for comparison. LSNF powder prepared by GNP has the same crystal structure as $LaFeO_3$. It is also similar with those prepared by traditional solid-state reaction, for example, reported by Chiba et al. [8]. However, the peaks as shown in Fig. 2 are much broader than those from solid-state reaction, indicating very small particle size of LSNF prepared by GNP comparing to that by solid-state reaction. The firing temperature to form the perovskite structure LSNF prepared by GNP is much lower (900 °C) than the traditional solid-state reaction (1200 °C) [8].

The electrical conductivity measured by four-probe technique is plotted in Fig. 3 as a function of temperature. At 800 °C, the conductivity of sample b is 146.7 S/cm, which is much lower than 340.9 S/cm for sample a. However, it should be noticed that the porosity of sample b is about 34%, which is the reason for the lower conductivity compared to the well-sintered LSNF (porosity <3%).

For practical use, the porosity of a cathode should be higher than 30%, and this value (146.7 S/cm) is high enough to use for current collection.

3.2. Microstructure characterization and AC impedance spectroscopy

A number of different sintering conditions were investigated. Results show that highly porous electrodes were obtained when sintering temperature was below 1000 °C, whereas the cathodes became too dense for sintering temperatures higher than 1000 °C. For example, LSNF sintered at 950 °C for 5 h (Fig. 4a and b) showed a structure with reasonable porosity and well-necked particles. The pore sizes appeared to be 100–200 nm. Shown in Fig. 5 is the plot of Area Specific Resistance (ASR) of LSNF measured at 750 °C in air as a function of the sintering temperature ranging form 850 to 1150 °C at an interval of 50 °C. ASR is one half of the difference between the real-axis intercepts of the impedance plots and corrected for area since the impedance was measured on symmetric cells. The lowest ASR was achieved for cathodes sintered at 950 °C. The sintering behavior of LSNF–SDC composites was similar to that of LSNF, and the interfacial resistance for LSNF–SDC composite cathodes was the lowest when the electrodes were sintered at 950 °C for 5 h.

A typical impedance spectroscopy for an LSNF–SDC cathode at various temperatures is shown in Fig. 6. At temperatures higher than 700 °C, an obviously additional arc appeared at low frequency that was independent of temperature. It is found that the contributions from the two arcs were approximately equal at 750 °C, and at higher temperatures the low-frequency arc dominated. The low-frequency arc, which is found to be insensitive to temperature, is there-

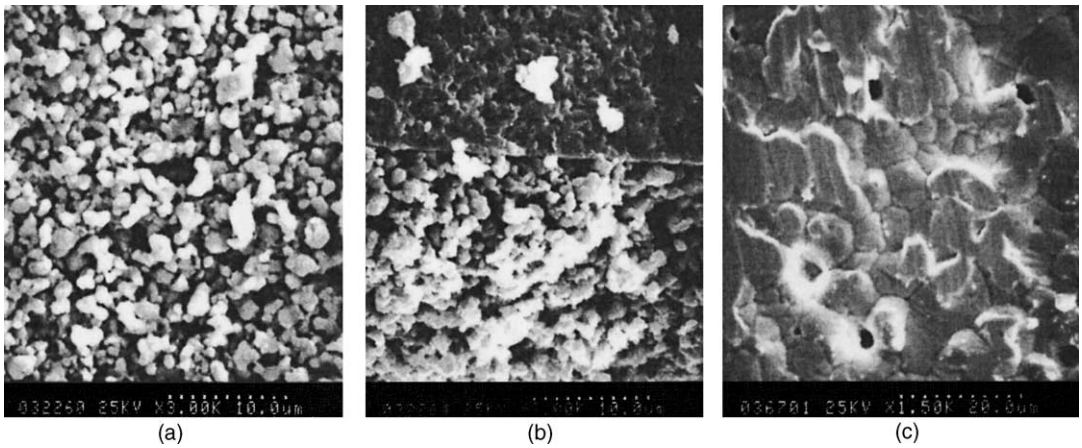

Fig. 4. SEM images of LSNF sintered at 950 °C for 5 h (a, b) and Ag paste fired at 700 °C for 5 h (c).

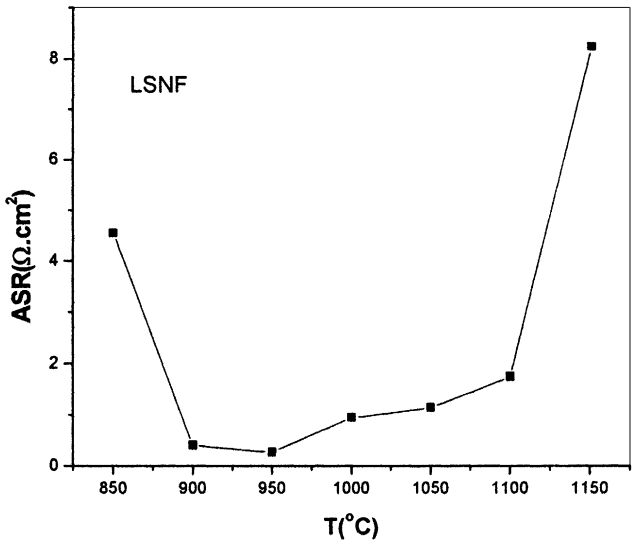

Fig. 5. Area Specific Resistance (ASR) of the LSNF measured at 750 °C in air as a function of the sintering temperature.

fore ascribed to gas diffusion. Shown in Fig. 4c is the SEM of Ag paste used as current collector with little porosity. It is likely that the current collector with little porosity blocks gas diffusion. At lower temperature, significant overlap was observed, giving the appearance of a single depressed arc. Attempts were made to fit the impedance arcs, however, overlapping of the arcs made it difficult to deconvolute the impedance spectroscopy with reasonable accuracy. In this work, the low-frequency arc became more dominant with increasing temperature, which typically indicates that the primary rate-limiting mechanism is diffusion related. Fortunately, the influence of gas diffusion can be reduced by optimizing the microstructure of the electrode.

Shown in Fig. 7 is the temperature dependence of the low-current polarization resistance ASRs for pure LSNF and LSNF–SDC composite. In general, ASR decreased as SDC concentration increased up to 50 wt.%. Further increased SDC content results in the increasing of the interfacial resistance. The effect observed was clearly shown in Fig. 8, where the ASR is plotted as a function of SDC volume fraction. The curve shows the ASR of composite cathode dramatically drop for a microstructure in which SDC content is around at 45 vol.%. It is ∼5 times lower than those for the LSNF and other LSNF–SDC composite cathodes. Incorporating the effects of porosity and particle size ratio we think the percolation threshold of this system is around 45%. The apparent activation energy of LSNF–SDC50 cathode is 1.22 eV over a temperature range of 500–700 °C. However, at temperature above 750 °C, the apparent activation energy becomes smaller. It is because gas diffusion which was independent of temperature has been become the primary rate-limiting step. When SDC content increases from 50 to 53 wt.%, ASR sharply increases and the substantially lower activation energy for LSNF–SDC53 (1.13 eV), which sug-

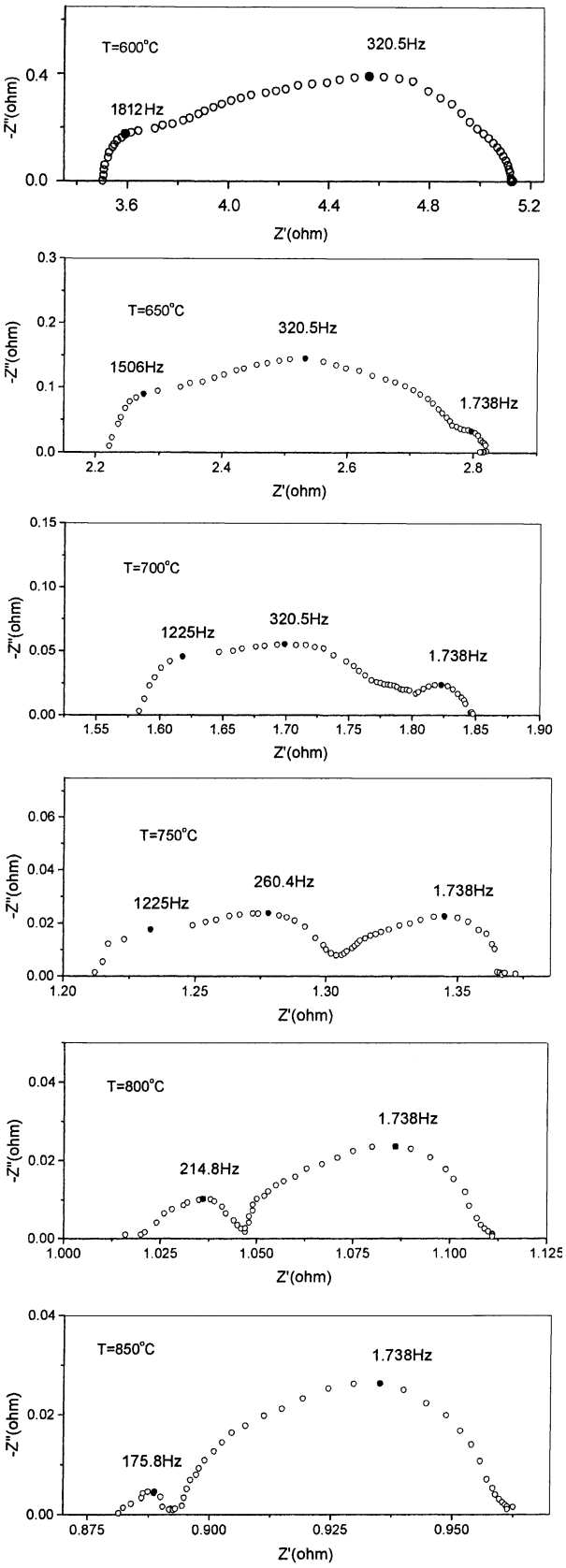

Fig. 6. Impedance spectroscopy for an LSNF–SDC50 cathode in air at various temperatures.

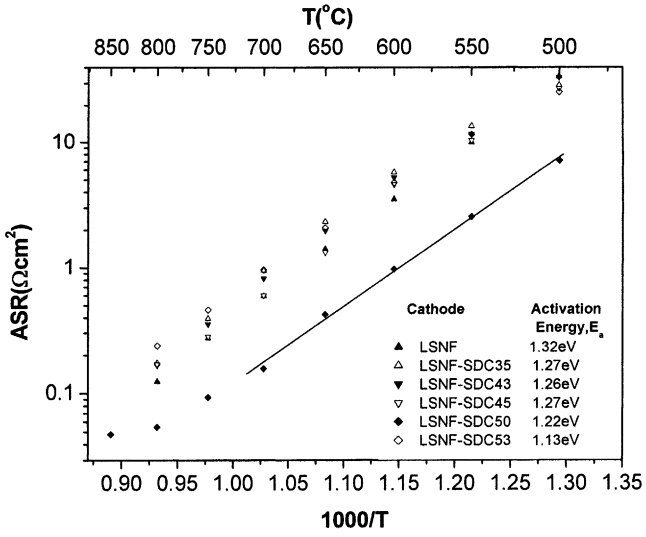

Fig. 7. Arrhenius plot of Area Specific Resistance (ASR) for LSNF–SDC composite cathodes containing different amounts of SDC.

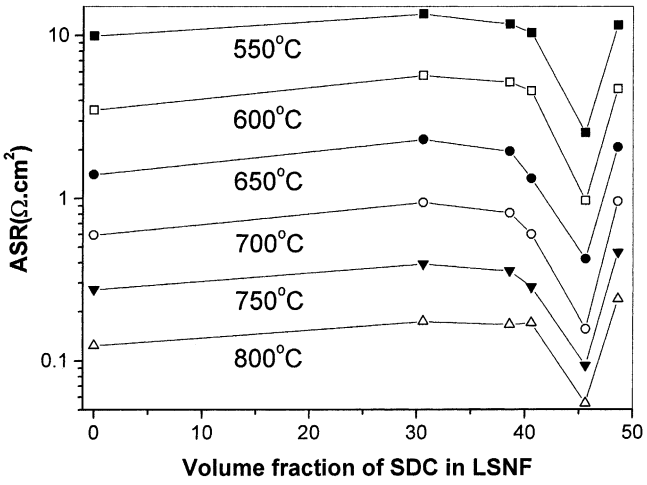

Fig. 8. Area Specific Resistance (ASR) of the two-phase system as a function of the volume fraction of SDC.

gests a different reaction mechanism was limiting in this case. At the same time, we should notice that the activation energy of pure LSNF cathode is 1.32 eV, which is slightly larger than that of composite cathodes. It should be the effect of the addition of SDC phase that has higher oxygen ion conductivity than LSNF. In a word, it is clear that the 50 wt.% LSNF/50 wt.% SDC was optimal, since there is approximately 5 times decrease in resistance.

4. Conclusions

The key result in the present work is the discussion of using $La_{0.4}Sr_{0.6}Ni_{0.2}Fe_{0.8}O_3$ as cathode for intermediate temperature SOFCs, the factor of 5 reduction in the LSNF low-current interfacial resistance achieved by the addition of 45 vol.% SDC, for example, ASR is 0.16 $\Omega\,cm^2$ at 700 °C and 0.06 $\Omega\,cm^2$ at 800 °C. Note that contribution of gas diffusion, and these are low-current values, the ASR presumably decreases with optimizing microstructure of electrode and increasing current density. It may be concluded that the percolation limit for this system lies in around 45 vol.% SDC. A few mechanisms may explain the enhanced electrode performance produced by the SDC addition. However, it seems likely that the high-ionic conductivity of SDC played a key role by expanding the electrochemical reaction zone further form the electrode/electrolyte interface. We also investigated the temperature dependence of the electronic conductivity when the sample has 34% porosity; its conductivity (145.7 S/cm at 800 °C) is high enough as current collector.

Acknowledgements

The authors gratefully acknowledge the financial support of the Ministry of Science and Technology of China under award No. 2001AA323090, and Nature Science Foundation of China under award No. 50372066.

References

[1] N.Q. Minh, J. Am. Ceram. Soc. 76 (3) (1993) 563.
[2] H.Y. Tu, Y. Takeda, N. Imanishi, O. Yamamoto, Solid State Ionics 117 (1999) 277.
[3] S.C. Singhal, Proc. 3rd Int. Symp. SOFC, vol. 93-4, The Electrochemical Society, Inc., 1993, p. 665.
[4] M. Juhl, S. Primdahl, C. Manon, M. Mogensen, J. Power Sources 61 (1996) 173.
[5] O. Yamamoto, Y. Takeda, R. Kanno, M. Noda, Solid State Ionics 22 (1987) 241.
[6] S.P. Simner, J.F. Bonnett, N.L. Canfield, K.D. Meinhardt, J.P. Shelton, V.L. Sprenkle, J.W. Stevenson, J. Power Sources 113 (2003) 1.
[7] M. Hrovat, N. Katsarakis, K. Reichmann, S. Bernik, D. Kuscer, J. Hole, Solid State Ionics 83 (1996) 99.
[8] R. Chiba, F. Yoshimura, Y. Sakurai, Solid State Ionics 152/153 (2002) 575.
[9] R. Chiba, F. Yoshimura, Y. Sakurai, Solid State Ionics 124 (1999) 281.
[10] A.S. Mukasyan, C. Costello, K.P. Sherlak, D. Lafarga, A. Varma, Sep. Purif. Technol. 25 (2001) 117.
[11] Y. Gu, G. Li, G. Meng, D. Peng, Mater. Res. Bull. 35 (2000) 297.